

Ammonia adsorption on and diffusion into thin ice films grown on Pt(111)

T. Takaoka, M. Inamura, S. Yanagimachi, I. Kusunoki,^{a)} and T. Komeda

Institute of Multidisciplinary Research for Advanced Materials, Tohoku University, Katahira 2-1-1, Aoba-ku, Sendai 980-8577, Japan

(Received 29 December 2003; accepted 2 June 2004)

Ammonia adsorption on and diffusion into thin ice films grown on a Pt(111) surface were studied using Fourier transform infrared spectroscopy (FTIR) and thermal desorption spectroscopy. After exposing the crystalline ice film to ammonia molecules at 45 K (ammonia/ice film), we have detected an intriguing feature at 1470 cm^{-1} in the FTIR spectra, which is derived from the adsorption of ammonia on the ice with a characteristic structure which appears in thin film range. The peak intensity of this feature decreases gradually as the thickness of the substrate ice increases. In addition, we have detected a feature at 1260 cm^{-1} which appears after annealing the ammonia/ice film. The feature corresponds to the ammonia molecules which reach the ice/Pt(111) interface through the ice film. Intriguingly, the intensity of this feature decreases with the ice thickness and there is a linear relation of the peak intensity of the features at 1470 and 1260 cm^{-1} . We propose a model in which the solubility of the ammonia molecules is much higher for the thin ice film than that for the ideal ice. © 2004 American Institute of Physics. [DOI: 10.1063/1.1775781]

I. INTRODUCTION

Water ice is one of the most abundant molecular solids in nature, and consequently, the interaction between water ice and molecules is a topic of interest and research in various fields of science^{1–3} such as atmospheric chemistry,^{4–6} chemical evolution in space,⁷ and life science.⁸ To understand the ice-adsorbate interactions in a wide variety of scientific disciplines in this context, molecular level investigation is necessary. For that purpose the well-defined ice surface prepared on metal surfaces under ultrahigh vacuum condition is a good target, since clean ice film without impurity can be grown and its crystallinity can be controlled by adjusting several parameters. Thin ice film grown on Pt(111) surface has been studied, in particular, on which water molecules adsorb molecularly.^{1,9–12} However, the various nature of the thin ice film is still left unknown.

Hexagonal I_h and cubic I_c are known as crystalline ice structures under atmospheric pressure;¹³ in both structures the crystalline ice has a layered structure and water molecules form hexagonal rings with three lying in the lower plane and three in the upper one, which is commonly called as a bilayer (BL) arrangement.

For thin film ice structure on Pt(111) surface, the results of He scattering experiment have shown formation of the well-ordered two-dimensional (2D) ice with a $(\sqrt{37} \times \sqrt{37})$ R25.3° symmetry in prior to the formation of 1 BL, after which the ice film rotates to give a $(\sqrt{39} \times \sqrt{39})$ R16.1° structure.¹⁴ The former structure is expanded by 4% and the latter is compressed by 3% from that of the ideal ice crystal. In the studies of low-energy electron diffraction (LEED) experiments, ice structures are observed.^{15–17} It has been reported that the $(\sqrt{39} \times \sqrt{39})$ R16.1° structure in the thickness

region of 1–4 BL changes to that of ideal ice crystal above that thickness.¹⁷ The images of scanning tunnel microscope observation show the mixture of several phases of ice structures, which are slightly deformed from the $(\sqrt{3} \times \sqrt{3})$ R30° structure; examples can be seen on Pt(111) at 120–140 K.^{18,19}

The presence of “free” OH atoms, which are not bound to the neighbor water molecules through hydrogen bonding, is also an area of recent intensive researches. These free OH species have been detected with the Fourier transform infrared spectroscopy (FTIR), which interact with adsorbates like ammonia through H bonding.²⁰

From the demand for the understanding of atmospheric processes such as acid rain and the depletion of ozone layer, adsorption of gas molecules, which include CF_x , Cl_y , HNO_3 , HCl , N_2O_5 , on ice surface has been studied extensively.^{21,22} The ammonia molecules also play a crucial role in atmospheric chemistry in a sense that they form alkali species.²³ The interaction between ammonia molecules and ice surface has been reported by several groups.^{20,24–28} Reaction rates of the conversion of ice nanocrystals within 3D arrays to ammonia hydrates were measured by Uras and Devlin using transmission FTIR spectroscopy.²⁴ Bulk diffusion of a variety of molecules in ice and surface diffusion on ice were observed by Livingston *et al.* using laser resonant desorption techniques.²⁶

In this paper, adsorption and diffusion of ammonia molecules on thin ice film grown on Pt(111) surface are studied by using FTIR and thermal desorption spectroscopy (TDS). An intriguing ammonia induced feature is observed at 1470 cm^{-1} which gradually decreases when the thickness of the substrate ice film increases. The feature which corresponds to the ammonia molecules which reach the interface of ice/Pt(111) through the ice film after annealing appears at 1260 cm^{-1} , whose intensity shows a linear correlation with that of the feature at 1470 cm^{-1} . We propose a model that

^{a)}Present address: AYUMI INDUSTRY CO., LTD, Bessho Kagumachi 60, Himeji 671-0225, Japan.

the peak at 1470 cm^{-1} in FTIR spectra is a feature induced by the adsorption of ammonia on characteristic ice, whose structure is affected by the substrate. In addition ammonia adsorbed on such ice has much higher solubility than those adsorbed on the ideal ice due to the difference of the ice structure.

II. EXPERIMENT

The experiments were carried out in a homemade UHV chamber equipped with a Fourier transform infrared spectrometer (Nicolet, Magna 860), a quadrupole mass spectrometer for TDS, an Auger electron spectrometer (AES), LEED system, and a Bayard-Alpert ionization gauge. The chamber has a volume of 60 l and its pumping system is composed of a turbo molecular pump (1470 l/s), Ti sublimation pump, and a liquid nitrogen cold trap. The base pressure of the chamber is 2.0×10^{-10} Torr.

An FTIR system including a light source, a spectrometer, focusing mirrors, and a liquid N_2 cooled mercury-cadmium-telluride detector is combined with the UHV chamber. The optical path was purged with dry air or nitrogen gas. The incident angle of the infrared light to the sample was around 85° . FTIR spectra were measured with the resolution of 4 cm^{-1} , and a scan number from 500 to 1000.

A clean Pt(111) surface was prepared by Ne ion bombardment, a 1 min annealing at 1073 K, and a 1 L oxygen dose at 823 K to remove residual carbon atoms. The oxygen exposure was adjusted to prevent the excess oxygen remaining on the surface. After the procedure, AES and LEED showed the sample to be free of contaminants. A crystal temperature was measured with a chromel-alumel thermocouple spot welded on the side of the crystal. The sample was cooled by a contact with the head of a He cryostat.²⁹ The lowest temperature obtainable was 40 K. Heating rate during TDS measurements was 1 K/s. Both of annealing rate and cooling rate were also 1 K/s. The Pt(111) surface is exposed to water molecules via a tube doser positioned ~ 50 mm apart from the surface. Ammonia molecules are dosed by admitting ammonia vapor into the chamber.

III. RESULTS

Figures 1(a)–1(d) show the TDS spectra of H_2O ($m/e = 18$) from the Pt(111) surface exposed to water (H_2O) vapor. The dosing of the water vapor was executed at the substrate temperature of 137 K.

A single feature is identified for the small exposure region at the temperature of 170 K which is due to the water molecules directly adsorbed on the Pt(111) surface.

The peak intensity of the feature at 170 K is saturated at the exposure of 2.0 L (Langmuir; $1\text{L} = 1 \times 10^{-6}$ Torr sec), in which we assign the amount of the water molecule as 1 BL. For the exposures larger than 2.0 L, we can identify a second peak at the lower temperature region (150–160 K), which is assigned to the desorption of the water molecules in the second layer or above. The amount of the adsorbed water molecules is calibrated from the area of water peak ($m/e = 18$) in TDS spectra in this article.

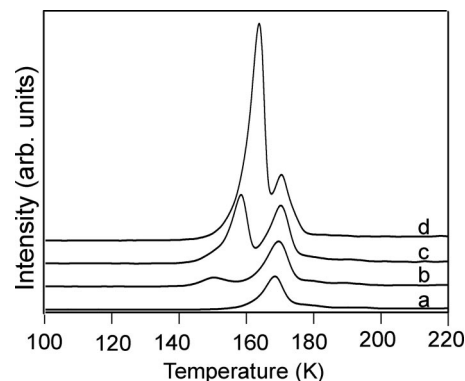


FIG. 1. TDS spectra of H_2O ($m/e = 18$) from the $\text{ice}_c/\text{Pt}(111)$ surface, where the Pt(111) surface is exposed to water vapor at the substrate temperature of 137 K. Ice film thickness is 0.7 (a), 1.2 (b), 1.9 (c), and 4.0 BL (d).

Figure 2 show FTIR spectra of the ice film of 4 BL grown on the Pt(111) surface, in which the ice film is prepared at the Pt(111) substrate temperature of 137 K [Fig. 2(a)], and 131 K [Fig. 2(b)] where the growth rate was kept at $\sim 0.02\text{ BL s}^{-1}$. Surface ordering of ice film was checked by comparing FTIR and TDS spectra with those reported in Ref. 17.

A broad band at $3000\text{--}3600\text{ cm}^{-1}$, which should be assigned to OH stretching modes of bulk ice, can be observed in both spectra. However, the peak shape in this energy range shows a quite large difference from each other, and it is quite intriguing that the difference of the growth temperature of a few Kelvin has a dramatic influence on the spectra. The origin has been deduced to the change of the structure from amorphous to crystalline. Following the understanding of the previous works, we assign the ice whose FTIR spectra corresponds to Figs. 2(a) and 2(b) to crystalline ice film [$\text{ice}_c/\text{Pt}(111)$] and amorphous ice film [$\text{ice}_a/\text{Pt}(111)$], respectively.³⁰ Unfortunately the setup of our LEED system is not adequate to observe the structure change directly.

Other features in the FTIR spectra should be assigned like following: (1) the peak at 3695 cm^{-1} as a stretching mode of free OH;³¹ (2) the peak at 1630 cm^{-1} as the HOH bending (ν_2 , scissoring) mode; (3) the shoulder around 1550 cm^{-1} as an overtone of a librational modes.³²

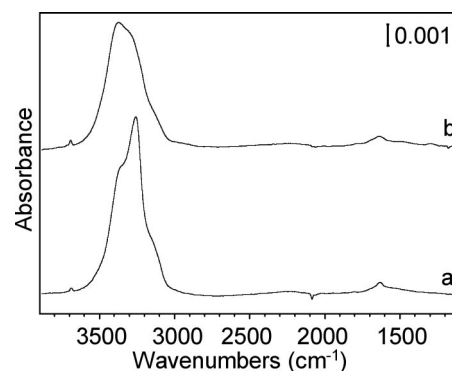


FIG. 2. FTIR spectra of the ice film of 4 BL grown on Pt(111) surface, in which the ice film is prepared at the Pt(111) substrate temperature of 137 K (a) and 131 K (b), respectively. The growth rate is kept at $\sim 0.02\text{ BL s}^{-1}$.

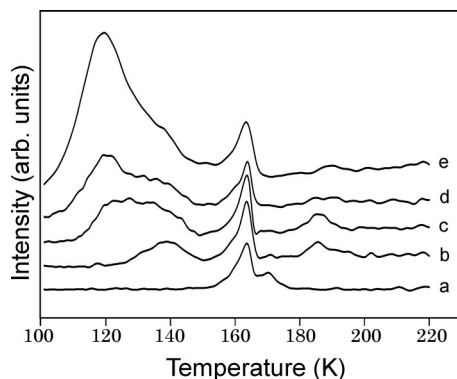


FIG. 3. TDS spectra of mass 16 ($m/e = 16$) from the ammonia/ice_c/Pt(111) surface, where the crystalline ice film with the thickness of 4 BL is exposed to ammonia vapor of 0 (a), 0.7 (b), 1.5 (c), 2.0 (d), and 4.0 L (e) at the substrate temperature of 45 K.

Next we show the TDS and FTIR spectra of the surface in which ammonia molecules are dosed on the ice formed on Pt(111) surface [ammonia/ice/Pt(111)].

Figure 3 show the TDS spectra of mass 16 ($m/e = 16$) from the ice film with the thickness of 4 BL exposed to 0, 0.7, 1.5, 2.0, and 4.0 L ammonia vapor at 45 K for (a), (b), (c), (d), and (e), respectively. Figure 4 show those of mass 18 ($m/e = 18$) from the 4 BL ice film exposed to 0, 0.7, 1.5, 2.0, and 4.0 L ammonia vapor at 45 K for (a), (b), (c), (d), and (e), respectively. As shown in Fig. 3(b), a broad peak is observed at 140 K for the exposure less than 0.7 L. When the exposure is more than 0.7 L, a new peak appears at around 120 K. Its intensity increases with increasing ammonia exposures. The peak is assigned to the desorption of multilayer or solid ammonia molecules.^{33,34} The peak at 140 K is assigned to the desorption of ammonia directly adsorbed on the ice surface. The reason of the assignment is as follows: first, the temperature of the peak is higher than that for multilayer ammonia; second, an FTIR peak corresponding to the free OH at the outermost surface of ice disappears after the ice surface is exposed to 0.7 L ammonia vapor.

Features observed in 150–180 K range in Fig. 3 are assigned to the fragment of water molecules. The reason of the assignment is as follows: (i) shape of the features is very similar to that in 150–180 K range for water TDS spectra

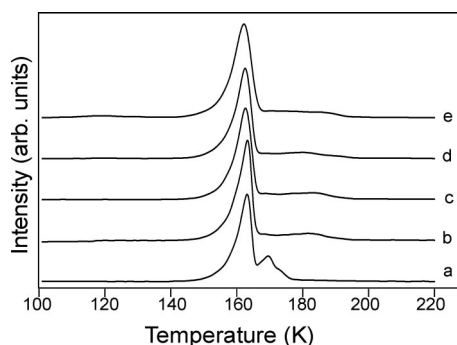


FIG. 4. TDS spectra of mass 18 ($m/e = 18$) from the ammonia/ice_c/Pt(111) surface, where the crystalline ice film with the thickness of 4 BL is exposed to ammonia vapor of 0 (a), 0.7 (b), 1.5 (c), 2.0 (d), and 4.0 L (e) at the substrate temperature of 45 K.

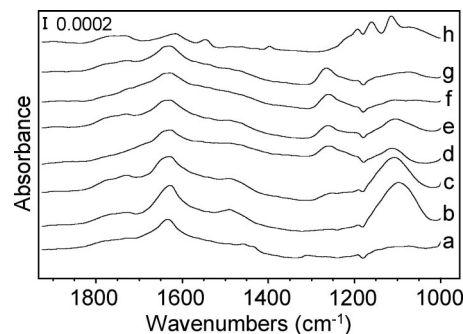


FIG. 5. FTIR spectra of the surface where the crystalline ice film of 4 BL on the Pt(111) surface is exposed to ammonia vapor of 4.0 L at 45 K (b) and subsequently flashed to 108 K (c), 118 K (d), 128 K (e), 138 K (f), 152 K (g), and 178 K (h), respectively. (a) spectrum of the 4 BL ice film without ammonia molecules for comparison.

(mass 18) obtained at the same time (Fig. 4); (ii) the intensity ratio between the features in 150–180 K range in mass 16 spectra (Fig. 3) and those in mass 18 spectra (Fig. 4) is identical with the previously reported data for water; (iii) the intensity of the features in 150–180 K range is almost the same for all of the spectra shown in Fig. 3, while the ammonia exposure increases from 0 L [Fig. 3(a)] to 4.0 L [Fig. 3(e)]. However, the features possibly include a small amount of ammonia molecules desorbed with water. If we had observed mass 15 spectra, we could have obtained TDS spectra of ammonia molecules without water fragment. However, we did not observe the mass 15 spectra since the intensity of the features in mass 15 spectra was very weak and we could not obtain a good S/N ratio in the spectra.

A peak around 185 K in Figs. 3(b)–3(e) is assigned to ammonia molecules remaining on the Pt(111) surface after the desorption of ice in 150–180 K range. However, we could not estimate the amount of the ammonia molecules.

The water TDS curves shown in Fig. 4 demonstrate that the presence of ammonia molecules changes the water desorption behavior. In Fig. 4(a) spectrum, peaks at 170 K and 160 K correspond to the desorption of first water bilayer and that of multilayers, respectively. In the spectra obtained after the ice surface is exposed to ammonia vapor, first water bilayer peak disappears [Figs. 4(b)–4(e)]. The cause of the disappearance is that water molecules directly bonded to Pt(111) surface are replaced by ammonia molecules during the heating process. Small features at 180–200 K in Figs. 4(b)–4(e) is assigned to the desorption of water molecules stabilized with the coadsorption with ammonia molecules on Pt(111) surface.

The FTIR spectrum for the surface where the ammonia vapor of 4.0 L is dosed at 45 K on the crystalline ice film of 4 BL is shown in Fig. 5(b); the spectrum of the substrate ice film is shown in Fig. 5(a) for comparison. The difference spectrum is shown in Fig. 6(a).

The spectral change in the region of 3000–3600 cm^{-1} in the spectrum shown in Fig. 6(a) is due to the appearance of vibrational modes of ammonia and the change of the ice film itself; namely, the protrusions at 3230 and 3380 cm^{-1} are assigned to NH stretching modes of ammonia molecules, and the dips in the range of 3400–3600 cm^{-1} are mainly due to

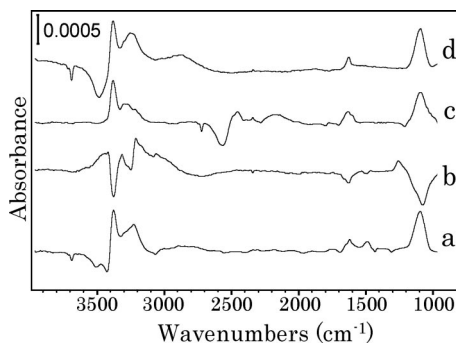


FIG. 6. FTIR difference spectra. (a) The spectrum obtained by subtracting the spectrum of $\text{ice}_c/\text{Pt}(111)$ surface [Fig. 5(a)] from that of ammonia/ $\text{ice}_c/\text{Pt}(111)$ surface [Fig. 5(b)]. (b) The spectrum obtained by subtracting the spectrum of ammonia/ $\text{ice}_c/\text{Pt}(111)$ surface before flashing [Fig. 5(b)] from that after flashing to 118 K [Fig. 5(d)]. (c) The spectrum obtained by subtracting the spectrum of $\text{ice}_c/\text{Pt}(111)$ surface from that of ammonia/ $\text{ice}_c/\text{Pt}(111)$ surface for deuterated ice (D_2O). The ammonia/ $\text{ice}_c/\text{Pt}(111)$ surface was prepared by exposing the crystalline deuterated ice film of 4 BL on the Pt(111) surface to ammonia vapor of 4.0 L at 45 K. Both spectrum of the $\text{ice}_c/\text{Pt}(111)$ surface and that of the ammonia/ $\text{ice}_c/\text{Pt}(111)$ surface for deuterated ice were observed at 45 K. (d) The spectrum obtained by subtracting the spectrum of the $\text{ice}_a/\text{Pt}(111)$ surface from that of the ammonia/ $\text{ice}_a/\text{Pt}(111)$ surface. The ammonia/ $\text{ice}_a/\text{Pt}(111)$ surface was prepared by exposing the amorphous ice film with 4 BL thickness on the Pt(111) surface to ammonia vapor of 4.0 L at 45 K. Both the spectrum of the $\text{ice}_a/\text{Pt}(111)$ surface and that of the ammonia/ $\text{ice}_a/\text{Pt}(111)$ surface for ice were observed at 45 K.

the change of the structure of the ice film or the change of the bonding state of water molecules in the ice film.^{27,28,35} The dip at 3695 cm^{-1} corresponds to the decrease of the free OH on the ice surface due to the hydrogen bonding with the ammonia molecules.²⁰ A peak at around 1630 cm^{-1} is assigned to ν_4 (asymmetric deformation) mode of ammonia molecules. The peak position is almost the same as that of the bending (ν_2 , scissoring) mode of water molecules. The peak at 1100 cm^{-1} is assigned to ν_2 (symmetric deformation; umbrella) mode of ammonia molecules. The peak observed at 1470 cm^{-1} will be described later.

Figures 5(c)–5(h) show FTIR spectra observed after the 4 BL crystalline ice is exposed to ammonia vapor at 45 K, flashed to various temperatures and subsequently cooled to 45 K. In the spectrum obtained after the flashing to 108 K [Fig. 5(c)], a new peak is observed at $\sim 1260\text{ cm}^{-1}$. With increasing flashing temperature, the intensity of the peak increases [Figs. 5(d)–5(g)]. The difference spectrum of before flashing [Fig. 5(b)] and after flashing to 118 K [Fig. 5(d)] is shown in Fig. 6(b), where the peak at 1260 cm^{-1} is visible more clearly. The dips at 1100, 1630, 3250, and 3390 cm^{-1} are due to desorption of multilayer ammonia molecules.

As far as we know, the peak at $\sim 1260\text{ cm}^{-1}$ has not been assigned to any vibrational modes of ammonia gas, liquid, solid, aqueous, ammonia-water cluster, and crystal.^{36–40}

We have obtained a similar feature in the FTIR spectra where the molecules of ammonia and water are dosed with the reverse order, i.e., the Pt(111) surface is exposed to 0.1–4.0 L ammonia vapor and subsequently to 4 L water (ice/ammonia/Pt(111) film) at 100 K. Features are observed in the range of $1250\text{--}1300\text{ cm}^{-1}$ for this system and the energy

considerably corresponds to the ammonia symmetric deformation mode. The peak at $\sim 1260\text{ cm}^{-1}$ is also observed in FTIR spectra obtained after the D_2O crystalline ice is exposed to ammonia vapor at 45 K and subsequently flashed.

It is quite possible that the peak at 1260 cm^{-1} corresponds to the vibrational mode of ammonia molecules which reach the ice/Pt(111) interface through the ice film. Similar scenario can be seen in Ref. 20, in which 1200 cm^{-1} peak is assigned to ammonia molecules exist in the interface between the ice and the Ru(001) surface.

Flashing to higher temperature induces the desorption of the substrate ice. The spectrum of Fig. 5(h) is obtained after the flashing to 178 K where water desorption is almost completed judged from the TDS spectra. Several peaks in the region of $1000\text{--}1250\text{ cm}^{-1}$ is assigned to ν_2 (umbrella) mode of ammonia molecules on the Pt(111) surface. Remaining of ammonia molecules on the surface after flashing to 178 K corresponds to the existence of the peak around 185 K in TDS spectra [Figs. 3(b)–3(e)].

IV. DISCUSSION

As shown above, we have detected characteristic features at 1470 cm^{-1} and 1260 cm^{-1} in FTIR spectra which should be connected with the ammonia adsorption on the ice film and penetration into it. Hereafter we further discuss the both features in detail.

A. Assignment of 1470 cm^{-1} peak in FTIR spectra

As shown in Fig. 5(b), the feature at 1470 cm^{-1} is observed when the crystalline ice surface is exposed to the ammonia vapor at 45 K. However, the feature cannot be detected when the ice film is replaced with D_2O film. The difference spectrum is shown in Fig. 6(c). This isotope experiment using D_2O shows that the feature is derived not solely by the ammonia molecule. Instead, the involvement of the substrate ice film on the appearance of this feature is indicated.

We can consider two possible assignments for the 1470 cm^{-1} feature: (1) the asymmetric deformation mode of ammonium ions (NH_4^+) which are formed by the proton transfer from the ice film to the NH_3 ; (2) the frequency shift of the vibrational mode of the ice film induced by the adsorption of the NH_3 .

We first discuss the asymmetric deformation mode of ammonium ions (NH_4^+). In the report of the FTIR observation of ammonia(NH_3)/ice(H_2O)/Ru(001) surface, the feature at 1470 cm^{-1} is observed when the surface is annealed at 120 K and is assigned to the asymmetric deformation mode of ammonium ions.²⁰ However, the peak is observed after the ice film is exposed to ammonia vapor even at 45 K in our experiment. This difference is probably caused by the difference of procedures to prepare the ice film. In Ref. 20, the ice film is deposited on Ru(001) surface below 100 K, and subsequently annealed at 125 K. In our experiment, the crystalline ice film is prepared at 137 K. When the ice film is prepared at 131 K, the feature is observed only after flashing the ammonia/ice film to 100 K.

If the NH_4^+ ion is formed by proton transfer between ammonia molecules, then the isotope experiment shown above cannot be accounted for. Thus the ion should be formed by the interaction between ammonia molecule and the ice surface. In case D_2O ice surface is used, deuterated ammonium ion will be produced. A theoretical calculation has reported that fundamental frequencies of deuterated ammonium ion except ND_4^+ are expected at the frequencies between $1400\text{--}1500\text{ cm}^{-1}$.⁴¹ Features at the frequencies between $1400\text{--}1500\text{ cm}^{-1}$ have been reported for a deuterated ammonium ion compound.⁴² In the spectrum shown in Fig. 6(c), no peaks are observed in the frequency range. However, there is some possibility of that H/D randomizing spreads the intensity of any bands all over the spectrum and no peaks are observed in the range. Thus the feature of 1470 cm^{-1} is possibly originated from the deformation mode of ammonium ions (NH_4^+).

On the other hand, the 1470 cm^{-1} feature can be also the ν_2 (scissoring) mode of water, the energy shift of which from the one on the pure ice film can be attributed to bonding with ammonia molecules. It is well known that intermolecular hydrogen bonding causes the shift to higher frequencies from the gas-phase value (1595 cm^{-1}). In addition, water ν_2 mode at around 1470 cm^{-1} has not been reported for $\text{NH}_3 \cdot x\text{H}_2\text{O}$ compounds ($x = 1/2, 1, 2$) and $\text{NH}_3 \cdot \text{H}_2\text{O}$ cluster as far as we know.^{36,37,39,40} However, frequencies between $1440\text{--}1520\text{ cm}^{-1}$ have been reported on metal surface, and in some compounds.^{1,43–45} The cause of the lower frequency shift has been proposed as the charge transfer from the $3a_1$ orbital of water which affects the scissoring mode force constant,¹ Fermi resonance between the scissoring mode and the overtone of the librational modes,⁴³ arrangement of the proton acceptors around the water molecules (bifurcated hydrogen bonds),⁴⁴ and coupling bending motion of water molecules which form water-metal chains.⁴⁵ Then, when ammonia molecules adsorb on the ice surface, bifurcated hydrogen bonds may be formed, or the shift of water librational mode may lead to the enhancement of the Fermi resonance between the scissoring mode and the overtone of the librational modes.

If this is the case, we can examine the isotope effect by using the combination of ammonia(ND_3)/ice_c(H_2O)/Pt(111) surface where ND_3 is adsorbed on crystalline water ice surface; the feature at 1470 cm^{-1} should be seen for this system also. However, this experiment is hampered by the existence of impurity ND_2H molecules which gives a peak at 1460 cm^{-1} which cannot be distinguished from the one of our interest.

On the ice with the thickness of 4–20 BL, the feature at 1470 cm^{-1} can be observed only on the crystalline ice; i.e., prepared at 137 K as noted above. Figures 6(a), and 6(d) show difference spectra of ammonia adsorbed on crystalline ice surface [ammonia/ice_c/Pt(111) surface], and that on amorphous ice surface [ammonia/ice_a/Pt(111) surface], respectively. The thickness of the ice film is 4 BL for both cases, and the spectra are obtained by subtracting the spectra of the pure ice from those obtained after ammonia dosing. The feature at 1470 cm^{-1} is observed only in the spectrum of ammonia/ice_c/Pt(111) [Fig. 6(a)], and not in that of

ammonia/ice_a/Pt(111) [Fig. 6(d)]. Although we cannot decide whether the feature at 1470 cm^{-1} is derived from the deformation mode of ammonium ion or frequency shifted scissoring mode of water as discussed above, it is demonstrated that the appearance of the feature is related to the structure or properties of ice surface.

Figure 7(a) shows the dependence of the intensity of the 1470 cm^{-1} peak [$I(1470)$] on the thickness of crystalline ice film. In the figure, it is clearly shown that the $I(1470)$ decreases with the increase of the ice thickness. We can explain the dependence by considering that the adsorption of ammonia on the area of ice, whose surface structure is different from that of ideal crystalline ice, induces the 1470 cm^{-1} peak, and the area decreases with increasing ice film thickness. It has been reported that the position of oxygen atoms of water molecules is well ordered with a complete bilayer (1×1) surface termination (ideal crystalline ice) in thick ice layers ($\sim 100\text{ \AA}$).⁴⁶

It is noted that no vibrational modes are reported in the frequency range of $\sim 1470\text{ cm}^{-1}$ in the simulation for ammonia molecules adsorbed on an optimized hexagonal ice (0001) film which is not affected by substrate.^{47,48}

B. Thickness dependence of ammonia diffusion

When the ammonia/ice_c/Pt(111) surface is heated, the peak is clearly observed at 1260 cm^{-1} in FTIR spectra as shown in Fig. 6(b). The peak is assigned to the vibrational mode of ammonia molecules which reach the ice/Pt(111) interface through the ice film. The thickness dependence of the intensity of the 1260 cm^{-1} peak [$I(1260)$] is shown in Fig. 7(b). $I(1260)$ in the figure is obtained after flashing ammonia/ice_c/Pt(111) surface to 113 K. As shown in the figure, the $I(1260)$ decreases with increasing the ice film thickness. It is confirmed that the ice surface is covered with ammonia molecules or ammonium ions during this experiments by observing no peaks corresponding to free OH at ice surface in the FTIR spectrum and by observing desorption peak of ammonia directly bonding to the ice surface in the TDS spectrum [Fig. 3(b)] after flashing to 113 K. Hence, the intensity of the 1260 cm^{-1} peak is not limited by the amount of ammonia molecules or ammonium ions on the top most surface of the ice film since the ice surface is covered with them during the flashing.

As the origin of such thickness dependence, one might consider the kinetic effect of the diffusion of ammonia into the ice film. In case the dependence reflects the rate of the diffusion of ammonia in ice film. For thicker ice film, the rate for ammonia to reach the ice/Pt(111) interface through the ice film is slow. Then, the amount of the ammonia molecules transferred to the ice/Pt(111) interface after flashing in a certain time is smaller for the thicker ice film. However, since additional flashing cycles make almost no change, the data shown in Fig. 7(b) is practically in its equilibrium state. In addition, $I(1260)$ obtained after the sample temperature had been kept at 93 K for 4 h depends on the film thickness. In Fig. 7(c), $I(1260)$ obtained after ice film of 3, 8, and 13 BL is exposed to ammonia molecules and subsequently kept at 93 K is shown as a function of annealing time. It is con-

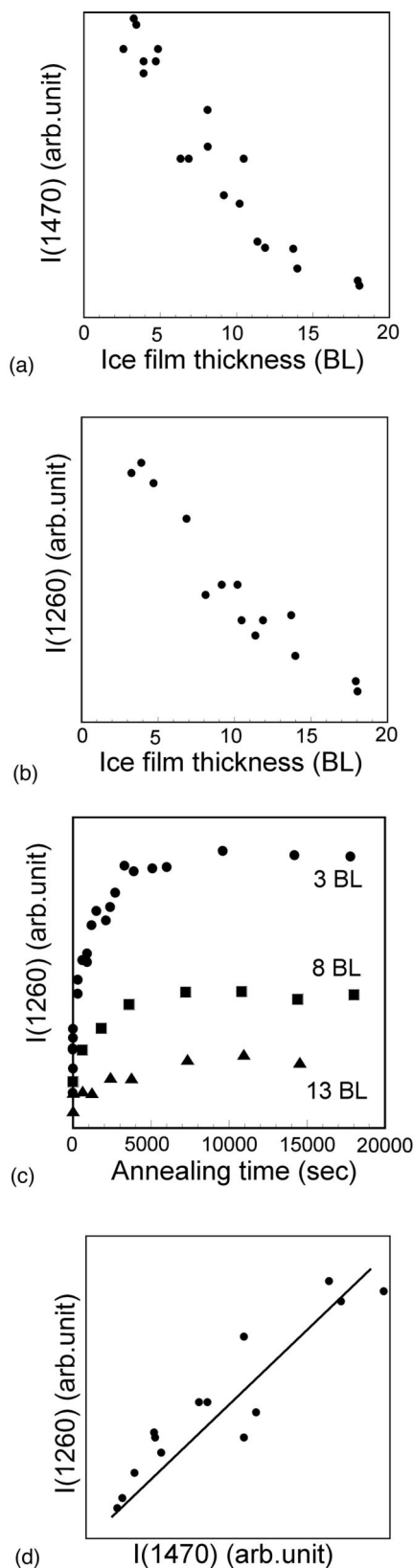


FIG. 7. (a) The intensity of the 1470 cm^{-1} peak [$I(1470)$] obtained after the $\text{ice}_c/\text{Pt}(111)$ surface is exposed to ammonia vapor at 45 K as a function of the thickness of the ice film. (b) The intensity of the 1260 cm^{-1} peak [$I(1260)$] obtained after the ammonia/ $\text{ice}_c/\text{Pt}(111)$ surface is flashed to 113 K as a function of the thickness of the ice film. (c) $I(1260)$ obtained after ice film of 3, 8, and 13 BL is exposed to ammonia vapor of 3.0 L and subsequently kept at 93 K is shown as a function of annealing time. (d) $I(1260)$ obtained after the ammonia/ $\text{ice}_c/\text{Pt}(111)$ surface is annealed to 113 K as a function of $I(1470)$ of the ammonia/ $\text{ice}_c/\text{Pt}(111)$ surface.

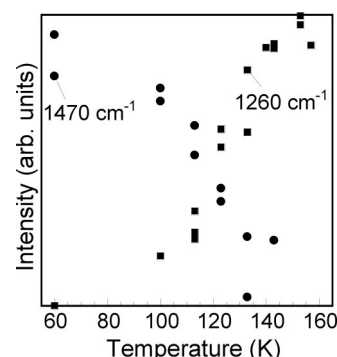


FIG. 8. Intensities of the 1260 cm^{-1} peak and the 1470 cm^{-1} peak for the ammonia/ $\text{ice}_c/\text{Pt}(111)$ surface with the ice film thickness of 4 BL as a function of flashing temperature.

firmed that the ice surface is covered with ammonia molecules or ammonium ions during this experiments. After about 2 h, $I(1260)$ is almost saturated, and the saturated value of $I(1260)$ depends on the film thickness. As the saturated value depends on the film thickness, the dependence is not caused by kinetic effect. These experimental results indicate that the amount of ammonia molecules, which can be transferred to the ice/ $\text{Pt}(111)$ interface after flashing to 113 K or annealing at 93 K, is limited to a certain value which decreases with increasing ice film thickness. We can understand this dependence by considering that the ice film is inhomogeneous, a region where ammonia can diffuse after the heating exists in the ice film, and the region decreases with increasing ice film thickness.

More interestingly there is a linear relation between $I(1260)$ and $I(1470)$, as shown in Fig. 7(d). This relation indicates that ammonia molecules, which lead to the appearance of the 1470 cm^{-1} peak upon adsorption, are considerably related to the diffusion of ammonia. In addition, $I(1470)$ and $I(1260)$ measured after ammonia/ $\text{ice}_c/\text{Pt}(111)$ is flashed to several temperatures are shown in Fig. 8, and it is found that $I(1260)$ increases with decreasing $I(1470)$. From these results, we consider that ammonia, which leads to the feature at 1470 cm^{-1} upon adsorption, diffuses into ice film and reaches the ice/ $\text{Pt}(111)$ interface upon flashing to 113 K or annealing at 93 K, i.e., it is an intermediate or a precursor of the diffusion of ammonia to the interface.

Based on the experimental results and the discussion about the features at 1470 and 1260 cm^{-1} , we can propose a model for adsorption and diffusion of ammonia molecules on ice films as follows: (i) ice film is inhomogeneous, and there is the region where ammonia can diffuse easily; (ii) the adsorption of ammonia molecules on the region leads to the appearance of the 1470 cm^{-1} peak; (iii) after flashing the film to 113 K or annealing at 93 K, ammonia can diffuse through the region and reach the ice/ $\text{Pt}(111)$ interface; (iv) the region decreases with increasing ice film thickness. Figure 9 is a schematic drawing of the model. In this schematic, it is assumed that the ammonia molecules or ammonium ions leading to the 1470 cm^{-1} peak are on the ice surface.

The appearance of the region where ammonia can diffuse after flashing to 113 K or annealing at 93 K is a characteristic feature of thin ice film on $\text{Pt}(111)$ surface. It is

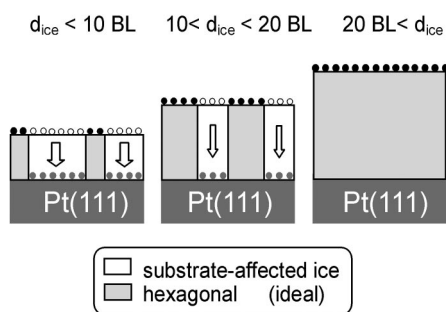


FIG. 9. A schematic drawing of the model discussed in the text. The region where ammonia can diffuse after flashing the film to 113 K or annealing at 93 K is denoted as “substrate-affected ice.” Open circles denote the ammonia molecules or ammonium ions on the region, which lead to the appearance of the 1470 cm^{-1} peak. In this schematic, it is assumed that the ammonia molecules or ammonium ions leading to the 1470 cm^{-1} peak are on the ice surface. Closed circles denote the ammonia molecules on the surface of hexagonal (ideal) ice. Shaded circles denote the ammonia molecules at the ice/Pt(111) interface, which lead to the appearance of the 1260 cm^{-1} peak. Arrows indicate the diffusion of ammonia molecules in the ice film.

known that the position of oxygen atoms of water molecules were found to be well ordered with a complete bilayer (1×1) surface termination in thick ice layers ($\sim 100\text{ \AA}$) prepared by exposing the Pt(111) surface to water at sample temperature of 125 K.⁴⁶ However, as there is a difference between lattice constant of Pt(111) surface and the corresponding ice lattice constant, the structure or property of ice in the 1–20 BL region is possibly different from that of crystalline bulk ice.

One of the features of thin ice film on Pt(111) surface can be the ordering of free OH species, which are not coordinated to other water molecules in the top-most ice layer. In I_h crystalline ice, free OH species are oriented randomly.^{1–3} On the other hand, a recent report on the first BL of ice on the Pt(111) surface claimed that free OH species are pointing down towards the surface (H down), which decreases the number of active sites and makes the ice film flat.¹⁰ Such differences of the orientation of the OH species should affect the adsorption and diffusion behavior of ammonia, since free OH plays an important role upon forming a hydrogen bond between ammonia and water.^{20,36,47,48} The ordering of OH is possibly maintained for thin ice film and lost for the surface of thick ice films. Harnett *et al.* have reported that there is no net proton ordering after 2 BL ice have grown, and this does not change in the 2–10 BL regime even for epitaxial thin ($\sqrt{39} \times \sqrt{39}$) R16.1° ice film formed on the Pt(111) surface.⁴⁹ It is therefore difficult to see how the surface OH orientation can change and influence ammonia adsorption.

The presence of the domain boundary can also be related to the appearance of the 1470 and 1260 cm^{-1} features. The existence of domain boundaries has been suggested between different phases or orientations of ice films with thickness of about 1000 \AA in the study using HAS technique.⁵⁰ The lattice constant of the domain is 2.1 times larger than that of ideally terminated surface of crystalline ice. It is possible that the 1470 cm^{-1} feature is originated from the domain boundary of ice film, and the area of which decreases with the increase of the film thickness. However, it is noted that there is no

evidence of the domain boundaries in the reported LEED experiment of thin ice films.⁴⁹

It has been reported that ammonia molecules diffuse into ice cleaving the bonding between the water molecules.²⁶ Then, penetration may occur easily for ammonia molecules in ice film with those structures distorted from the crystalline ice, since bonding between water molecules is probably unstabilized in those structures.

The feature at 1260 cm^{-1} is observed even at 83 K when the ammonia/ice_c(2 BL)/Pt(111) surface is annealed for 1 h. However the reported diffusion rate of ammonia molecules in the I_h ice at 83 K is very small. The diffusion coefficients for ammonia in hemihydrate have been determined from the analysis of reaction rate for the conversion of ice nanocrystals to hemihydrate of ammonia in the temperature range of 102–112 K.²⁴ The reports for the diffusion of ammonia in ice film on Ru(0001) surface by Livingston, Smith, and George give a consistent results.²⁶ The given numerical values are like following; the activation energy of 15 kcal/mol with the preexponential factor of $7 \times 10^{13}\text{ cm}^2/\text{s}$ for the amorphous hemideuterate, and the activation energy of 12 kcal/mol with the preexponential factor of $9 \times 10^7\text{ cm}^2/\text{s}$ for crystalline hemideuterate. Based on these numbers, we estimate the expected penetration depth of ammonia molecules in the ice film with the conditions of the temperature of 83 K and time length of 3600 s. The result indicates the penetration depth of 0.01 \AA , which is less than 1% of the 2 BL which we use for the substrate. This indicates that rate of the diffusion of ammonia in the region, where ammonia can diffuse after flashing to 113 K or annealing at 93 K, is very large compared to that in crystalline ice and amorphous ice.

C. Vibrational modes of ammonia in bulk ice

In Ref. 20, it has been reported that 1470 cm^{-1} feature is observed after heating the ammonia/ice/Ru(001) surface to 120 K, and it is assignable to the deformation mode of ammonium ion (NH_4^+) which diffuse in ice film and some of which adsorb on Ru(001) as a result of diffusion. However, we are not clear that the feature is derived from ammonium ion in ice film and diffusion of ammonia in ice film occurs in the form of ammonium ion, because the feature appears after the crystalline ice film is exposed to ammonia vapor at low temperatures (45 K), and no modes assignable to deuterated ammonium ions (NH_3D , etc.) are detected when D_2O ice film is exposed to ammonia (NH_3) vapor. On the other hand, if the diffusion of ammonia in ice film occurs in the form of ammonia molecule, features of ammonia molecule in ice film should be observed. However, we have not found any features which can be well separated from those of ammonia molecules on the ice film and at the ice/Pt(111) interface. Hence, we do not have clear answers to the form of ammonia in ice film at present.

V. CONCLUSIONS

We studied ammonia adsorption on and diffusion into the thin ice film grown on the Pt(111) surface with Fourier transform infrared spectroscopy and thermal desorption spectroscopy. We have found an intriguing feature at 1470 cm^{-1}

in the FTIR spectra obtained after the ice film is exposed to ammonia vapor at 45 K. The feature is assigned to the asymmetric deformation mode of ammonium ions, or the frequency shifted scissoring mode of water, and its peak intensity decreases with the increase of the thickness of the ice film. We have also detected a feature at 1260 cm^{-1} when the ammonia/ice film is annealed, which is considerably originated from the ammonia which penetrates into ice film and reaches the ice/metal interface. The peak intensity of this feature decreases with the increases of the ice film thickness. The peak intensity of the feature at 1470 cm^{-1} and the 1260 cm^{-1} for several values of ice film thickness shows a linear correlation. Based on these results, we propose a model for adsorption and diffusion of ammonia on the ice film as follows: (i) the ice film is inhomogeneous, and the region where ammonia can diffuse after flashing to 113 K or annealing at 93 K exists in the ice film; (ii) the adsorption of ammonia on the region, where ammonia can diffuse, leads to the appearance of the 1470 cm^{-1} peak; (iii) after the heating of the ammonia/ice film, ammonia on the region can diffuse into the ice film and reach the ice/Pt(111) interface; (iv) the region decreases with increasing ice film thickness.

The appearance of the region where ammonia can diffuse after the heating is a characteristic feature of thin ice film on Pt(111) surface. We consider this feature is related to the OH ordered structure or the domain boundary.

ACKNOWLEDGMENTS

This work was financially supported in part by grants in aids for scientific research on Priority Areas "Surface Chemistry of Condensed Molecules" from the Ministry of Education, Culture, Sports, Science, and Technology of Japan.

¹P. A. Thiel and T. E. Madey, *Surf. Sci. Rep.* **7**, 211 (1987).

²P. V. Hobbs, *Ice Physics* (Oxford University Press, New York, 1974).

³V. F. Petrenko and R. W. Whitworth, *Physics of Ice* (Oxford University Press, New York, 1999).

⁴S.-M. Fan and D. J. Jacob, *Nature (London)* **359**, 522 (1992).

⁵S. Solomon, *Rev. Geophys.* **37**, 275 (1999).

⁶F. Donine and P. B. Shepson, *Science* **297**, 1506 (2002).

⁷J. M. Greenberg, *Surf. Sci.* **500**, 793 (2002).

⁸P. L. Davis, J. Baardsnes, M. J. Kuiper, and V. K. Walker, *Philos. Trans. R. Soc. London* **357**, 927 (2002).

⁹S. Meng, L. F. Xu, E. G. Wang, and S. Gao, *Phys. Rev. Lett.* **89**, 176104 (2002).

¹⁰H. Ogasawara, B. Brena, D. Nordlund, M. Nyberg, A. Pelmenchikov, L. G. M. Pettersson, and A. Nilsson, *Phys. Rev. Lett.* **89**, 276102 (2002).

¹¹A. Michaelides, V. A. Ranea, P. L. de Andres, and D. A. King, *Phys. Rev. Lett.* **90**, 216102 (2003).

¹²P. J. Feibelman, *Phys. Rev. Lett.* **91**, 059601 (2003).

¹³D. Eisenberg and W. Kauzmann, *The structure and properties of water* (Oxford University Press, London, 1969).

¹⁴A. Glebov, A. P. Graham, A. Menzel, and J. P. Toennies, *J. Chem. Phys.* **106**, 9382 (1997).

¹⁵N. Materer, U. Starke, A. Barbieri, M. A. Van Hove, G. A. Somorjai, G.-J. Kroes, and C. Minot, *J. Phys. Chem.* **99**, 6267 (1995).

¹⁶N. Materer, U. Starke, A. Barbieri, M. A. Van Hove, G. A. Somorjai, G.-J. Kroes, and C. Minot, *Surf. Sci.* **381**, 190 (1997).

¹⁷S. Haq, J. Harnett, and A. Hodgson, *Surf. Sci.* **505**, 171 (2002).

¹⁸M. Morgenstern, T. Michely, and G. Comsa, *Phys. Rev. Lett.* **77**, 703 (1996).

¹⁹M. Morgenstern, J. Muller, T. Michely, and G. Comsa, *Z. Phys. Chem. (Munich)* **198**, 43 (1997).

²⁰H. Ogasawara, N. Horimoto, and M. Kawai, *J. Chem. Phys.* **112**, 8229 (2000).

²¹J. P. Devlin and V. Buch, *J. Phys. Chem.* **99**, 16534 (1995).

²²C. Girardet and C. Toubin, *Surf. Sci. Rep.* **281**, 1 (2001).

²³F. J. Dentener and P. J. Crutzen, *J. Atmos. Chem.* **19**, 331 (1994).

²⁴N. Uras and J. P. Devlin, *J. Phys. Chem. A* **104**, 5770 (2000).

²⁵N. Uras, V. Buch, and J. P. Devlin, *J. Phys. Chem. B* **104**, 9203 (2000).

²⁶F. E. Livingston, J. A. Smith, and S. M. George, *J. Phys. Chem. A* **106**, 6309 (2002).

²⁷L. Delzeit, M. S. Devlin, B. Rowland, J. P. Devlin, and V. Buch, *J. Phys. Chem.* **100**, 10076 (1996).

²⁸B. Rowland, N. S. Kadagathur, J. P. Devlin, V. Buch, T. Feldman, and M. J. Wojcik, *J. Chem. Phys.* **102**, 8328 (1995).

²⁹J. T. Yates, Jr., *Experimental Innovations in Surface Science* (Springer-Verlag, New York, 1998), p. 159.

³⁰W. Hagen, A. G. G. M. Tielens, and J. M. Greenberg, *Chem. Phys.* **56**, 367 (1981).

³¹B. Rowland and J. P. Devlin, *J. Chem. Phys.* **94**, 812 (1991).

³²A. H. Hardin and K. B. Harvey, *Spectrochim. Acta, Part A* **29**, 1139 (1973).

³³G. B. Fisher, *Chem. Phys. Lett.* **79**, 452 (1981).

³⁴J. M. Gohndrome, C. W. Olsen, A. L. Backman, T. R. Gow, E. Yagasaki, and R. I. Masel, *J. Vac. Sci. Technol. A* **7**, 1986 (1989).

³⁵T. Yamada, H. Okuyama, T. Aruga, and M. Nishijima, *J. Phys. Chem. B* **107**, 13962 (2003).

³⁶B. Nelander and L. Nord, *J. Phys. Chem.* **86**, 4375 (1982).

³⁷J. E. Bertie and J. P. Devlin, *J. Chem. Phys.* **81**, 1559 (1984).

³⁸S. Suzer and L. Andrews, *J. Chem. Phys.* **87**, 5131 (1987).

³⁹J. E. Bertie and M. R. Shehata, *J. Chem. Phys.* **81**, 27 (1984).

⁴⁰J. E. Bertie and M. R. Shehata, *J. Chem. Phys.* **83**, 1449 (1985).

⁴¹Jan M. L. Martin and Timothy J. Lee, *Chem. Phys. Lett.* **258**, 129 (1996).

⁴²A. Kruger and A. M. Heyns, *Vib. Spectrosc.* **14**, 171 (1997).

⁴³B. Soptrajanov, G. Jovanovski, and L. Pejov, *J. Mol. Struct.* **613**, 47 (2002).

⁴⁴B. Soptrajanov, V. Stefov, I. Kuzmanovski, G. Jovanovski, H. D. Lutz, and B. Engelen, *J. Mol. Struct.* **613**, 7 (2002).

⁴⁵A. Grodzicki and P. Piszczek, *J. Mol. Struct.* **443**, 141 (1998).

⁴⁶J. Brown, A. Glebov, A. P. Graham, A. Menzel, and J. P. Toennies, *Phys. Rev. Lett.* **80**, 2638 (1998).

⁴⁷Y. Hara, N. T. Hashimoto, and M. Nagaoka, *Chem. Phys. Lett.* **348**, 107 (2001).

⁴⁸N. T. Hashimoto, Y. Hara, and M. Nagaoka, *Chem. Phys. Lett.* **350**, 141 (2001).

⁴⁹J. Harnett, S. Haq, and A. Hodgson, *Surf. Sci.* **528**, 15 (2003).

⁵⁰A. Glebov, A. P. Graham, A. Menzel, and J. P. Toennies, *J. Chem. Phys.* **112**, 11011 (2000).